

Learning Bayes’ theorem with a neural network for gravitational-wave inference

Alvin J. K. Chua* and Michele Vallisneri†

Jet Propulsion Laboratory, California Institute of Technology, Pasadena, CA 91109, U.S.A.

(Dated: August 31, 2022)

We wish to achieve the Holy Grail of Bayesian inference with deep-learning techniques: training a neural network to instantly produce the posterior $p(\theta|D)$ for the parameters θ , given the data D . In the setting of gravitational-wave astronomy, we have access to a generative model for signals in noisy data (i.e., we can instantiate the prior $p(\theta)$ and likelihood $p(D|\theta)$), but are unable to economically compute the posterior for even a single realization of D . Here we demonstrate how a network may be taught to estimate $p(\theta|D)$ regardless, by simply showing it numerous realizations of D .

Introduction. In the Bayesian analysis of signals immersed in noise [1], we seek a representation for the posterior probability of one or more parameters that govern the shape of the signals. Unless the parameter-to-signal map (the *forward model*) is very simple, the analysis (or *inverse solution*) comes at significant computational cost, as it requires the stochastic exploration of the likelihood surface at a large number of locations in parameter space. Such is the case, for instance, of parameter estimation for gravitational-wave sources such as the compact binaries detected by LIGO–Virgo [2, 3]; here each likelihood evaluation requires that we generate the gravitational waveform corresponding to a set of source parameters, and compute its noise-weighted correlation with detector data [4]. Waveform generation is usually the costlier operation, so gravitational-wave analysts often utilize faster, less accurate waveform models [5, 6], or accelerated *surrogates* of slower, more accurate models [7].

Extending the analysis from the data we have to the data we might measure (i.e., characterizing the parameter-estimation prospects of future experiments) compounds the expense, since we need to explore posteriors for many noise realizations, and across the domain of possible source parameters. For concreteness, we price the evaluation of a single Bayesian posterior at $\sim 10^6$ times the cost of generating a waveform, and the characterization of parameter-estimation prospects at $\sim 10^6$ times the cost of a posterior. With current computational resources, this means that (for instance) accurate component-mass estimates only become available hours or days after the detection of a binary black-hole coalescence [8, 9], while any extensive study of parameter-estimation prospects must rely on less reliable techniques such as the Fisher-matrix approximation [10].

In this Letter, we show how one- or two-dimensional marginalized Bayesian posteriors may be produced using *deep neural networks* [11] trained on large ensembles of signal + noise data streams. (Specifically, we adopt *multilayer perceptrons* [12], although other architectures are likely to be viable.) The network for each source parameter or parameter pair takes as input a noisy signal, and instantly outputs an approximate posterior, represented either as a histogram or parametrically (e.g., as a

Gaussian mixture). We dub such networks PERCIVAL:¹ Posterior Estimation Results Computed Instantaneously Via Artificial Learning. Crucially, the *loss function* used in the training of these networks does not require that we actually compute the likelihood or posterior for each signal, but only that we provide the true source parameters. As long as the training set reflects the assumed prior distribution of the parameters and sampling distribution of the noise, the resulting posteriors approximate the correct Bayesian distribution—and indeed they achieve it asymptotically for very large training sets and networks.

In the gravitational-wave context, the training of PERCIVAL typically requires $\sim 10^9$ waveform evaluations (plus the computation of network weight gradients), which is $\sim 10^3$ times the cost of stochastically exploring the posterior for a single noisy signal. However, the costly training is performed *offline*; afterwards, the networks can perform inference on multiple signals with negligible execution times. The prompt generation of posterior parameter distributions for binary coalescence alerts [14] could be a worthy use of this speed (once suitable networks are trained, which we do not attempt here). Another potential application is the generation of effective proposal kernels to facilitate more detailed posterior analyses with Markov chain Monte Carlo methods [15]. Last, very rapid inference could also prove useful in the characterization of parameter-estimation prospects for next-generation detectors such as LISA [16].

The still somewhat hefty cost of training PERCIVAL can be offset significantly by pairing it with its forward counterpart ROMAN [17], which is essentially a neural network that has been fitted to the relevant waveform model in a reduced-order representation [18]. ROMAN (Reduced-Order Modeling with Artificial Neurons) takes as input a set of source parameters, and outputs in milliseconds the corresponding signal at high accuracy; it provides a conceptually cleaner alternative to the combined analysis framework comprising surrogate waveforms [19] and the likelihood compression technique known as *reduced-order quadrature* [20]. Being a neural network, ROMAN has ad-

¹ After the original achiever of the Grail [13].

ditional features such as analytic waveform derivatives and—more pertinently for this work—the generation of waveforms in large batches at next to no marginal cost. The latter allows us to fully exploit highly parallel GPU architectures to build training sets for PERCIVAL that are effectively infinite in size, which in turn grants immunity to the perennial deep-learning problem of overfitting.

Deep-learning techniques have gained popularity in the gravitational-wave community over the past two years, with the majority of efforts focused on applying *convolutional neural networks* [21] to the *classification* task of signal detection, specifically for transient signals from compact binaries in ground-based detector data [22–31]. They are also being investigated as detection tools for persistent signals from asymmetric neutron stars [32–35]. While the application of neural networks to the *regression* task of source parameter estimation is addressed in some of these papers [23, 24, 26, 27], there it is restricted to the recovery of pointwise estimates, and with a frequentist characterization of errors based only on the test set. However, near the completion of this manuscript, we learned of related work by Gabbard et al. [36], where a conditional variational autoencoder [37] is trained on parameter–noisy signal pairs to output samples from the Bayesian posterior. We expect that comparison between our method and theirs will offer useful insight.

Training neural networks to produce posteriors. We now describe our scheme to perform Bayesian posterior estimation using neural networks. A *perceptron classifier* is a network that takes a data vector D as input and outputs the estimated probabilities $q_i[D]$ that the input belongs to each member of a universal set of N disjoint classes $\{C_i\}$. The *Bayesian optimal discriminant* is the classifier that returns the posterior probabilities $p_i[D] \propto p(D|C_i)p(C_i)$, where $p(D|C_i)$ is the likelihood of D occurring in C_i , and $p(C_i)$ is the prior probability of C_i itself. It is a well-established result in the machine-learning literature that perceptron classifiers can approximate Bayesian optimal discriminants [38, 39] when they are trained on a population of inputs $\{D_j\}$ distributed according to $p(D|C_i)p(C_i)$. This is achieved by minimizing (over the network weights) the loss function $\sum_j \lambda(\mathbf{1}_i[D_j], q_i[D_j])$, where $\mathbf{1}_i$ is the indicator function of C_i , and λ is some vector distance on the space $[0, 1]^N$ (e.g., the squared ℓ^2 norm, or the discrete Kullback–Leibler divergence [40]).

Note that the above training procedure does not require computation of the actual posteriors $p_i[D_j]$, but only the ability to randomly draw classes C_i from the prior $p(C_i)$ and data vectors D_j from the conditional sampling distribution $p(D|C_i)$ (i.e., we need a *generative model* of the data). To move from classification to the computation of posterior densities for continuous parameters, we may simply define classes based on a binning of the parameter domain of interest; in other words, the network will then output histograms of the target posterior.

This coarse graining of parameter space highlights the relationship between classification and regression, but is not actually necessary for our scheme, since the network can instead output a parametric posterior representation (such as a Gaussian mixture) to be fed into an analogous loss function. Although histograms rapidly become impractical for marginalized posteriors in > 2 dimensions, the parametric approach extends more readily to the estimation of higher-dimensional posteriors.

Let us now explicitly derive the loss function used in our scheme. Consider a data model described by the continuous parameters $\vartheta := \{\theta, \phi\}$, with θ denoting the parameters for which we seek a posterior. We seek to minimize the statistical distance $\lambda(p, q)$ between the (marginalized) true posterior $p(\theta|D) = \int d\phi p(\vartheta|D)$ and the network-estimated posterior $q(\theta|D)$, integrated over the distribution of the data $p(D)$. If λ is the Kullback–Leibler divergence, we have the integrated distance

$$\int dD p(D) \left[\int d\theta p(\theta|D) \ln \frac{p(\theta|D)}{q(\theta|D)} \right]. \quad (1)$$

Using Bayes’ theorem on $p(\vartheta|D)$ and dropping the term containing $p(D, \vartheta) \ln p(\theta|D)$ (which is constant with respect to the network weights), we obtain the loss function

$$L := - \iint dD d\vartheta p(D, \vartheta) \ln q(\theta|D), \quad (2)$$

which can be approximated (modulo normalization) as a discrete sum over a notional training batch $\{(\vartheta_j, D_j)\}$:

$$L \simeq - \sum_j \ln q(\theta_j|D_j), \quad (3)$$

where, crucially, each ϑ_j is first drawn from the prior $p(\vartheta)$ before D_j is drawn from the conditional $p(D|\vartheta_j)$.

The summand in Eq. (3) is precisely the q -dependent term in the Kullback–Leibler divergence between the Dirac delta function $\delta(\theta - \theta_j)$ and $q(\theta|D_j)$. Likewise, if the network-estimated posterior is represented as a histogram $q_i[D]$, Eq. (3) simplifies to

$$L \simeq - \sum_{ij} \mathbf{1}_i[\theta_j] \ln q_i[D_j], \quad (4)$$

where $\mathbf{1}_i$ is now the indicator function of the i -th histogram bin. Eq. (4) is familiar to machine-learning practitioners, and is more commonly known as the cross-entropy loss for classification problems [11]. Finally, note that a derivation similar to the one above can also be given for the squared ℓ^2 distance $\int d\theta |p(\theta|D) - q(\theta|D)|^2$, resulting in an alternative (but less tractable) loss

$$L' \simeq - \sum_j \left[2q(\theta_j|D_j) - \int d\theta |q(\theta|D_j)|^2 \right]. \quad (5)$$

Leveraging reduced waveform representations. In gravitational-wave astronomy, the data D is usually a time or frequency series of strain h measured by the detector. For the transient signals observed by ground-based detectors, h is typically a vector of length $\lesssim 10^4$; this rises to $\lesssim 10^8$ for persistent LIGO–Virgo signals, or the mHz-band signals sought by future space-based detectors. Once the presence of a signal is established, Bayesian inference proceeds via the canonical likelihood

$$p(D|\theta) \propto \exp \left\{ \frac{1}{2} \langle h(\vartheta) - D | h(\vartheta) - D \rangle \right\}, \quad (6)$$

where $\langle \cdot | \cdot \rangle$ is a noise-weighted inner product that incorporates a power spectral density model for the detector noise (assumed to be Gaussian and additive).

As mentioned earlier, the generation of the waveform template $h(\vartheta)$ and the evaluation of the inner product are both computationally expensive, due to the complexity of relativistic modeling and the large dimension of the inner-product space. In the *reduced-order modeling* framework [18], we mitigate this cost by constructing a reduced basis for the (far more compact) template manifold embedded in the inner-product space, as well as a fast interpolant for the template model in this reduced representation. The neural network ROMAN [17] implements this interpolation, allowing Eq. (6) to be cast in the reduced but statistically equivalent form

$$p(\beta|\theta) \propto \exp \left\{ -\frac{1}{2} |\alpha(\vartheta) - \beta|^2 \right\}, \quad (7)$$

where the d -vectors $\alpha(\vartheta)$ and β are the projections of $h(\vartheta)$ and D , respectively, onto the reduced basis; furthermore, $\beta = \alpha(\vartheta_*) + \nu$ for the true source parameters ϑ_* and the (projected) noise realization $\nu \sim \mathcal{N}(0, I_d)$.

In this Letter, we give a demonstration of PERCIVAL by using the four-parameter, $d \simeq 200$ ROMAN network described in [17], which embodies the family of 2.5PN TaylorF2 waveforms [41] emitted by inspiraling black-hole binaries with aligned spins $\chi_{1,2} \in [-1, 1]$ and component masses $m_{1,2} \in [1.25, 10] \times 10^5 M_\odot$. The ROMAN templates are normalized to unit signal-to-noise ratio $\rho := |\alpha| = \sqrt{\langle h|h \rangle}$. Here, we vary signal amplitudes by setting $\alpha \rightarrow \rho\alpha$; our model parameters are then $\vartheta = (M_c, \eta, \chi_1, \chi_2, \rho)$, where the chirp mass M_c and symmetric mass ratio η are an alternative parametrization of the $m_{1,2}$ space. Large batches of ROMAN signals (with noise added as described after Eq. (7)) can be generated on a 2014 Tesla K80 GPU in ~ 0.1 s.

Example results. The marginalized posteriors on the full domain of the ROMAN model are nontrivial: they are highly multimodal at sub-threshold signal-to-noise ratios $\rho < 8$, and this persists even for $\rho \in [8, 16]$ due to correlations in the (η, χ_1, χ_2) space (although M_c is then better constrained). The parameter space is also quite large from a Fisher-information perspective, resulting in posteriors that are highly localized and hence difficult to resolve. We train a number of one- and two-dimensional

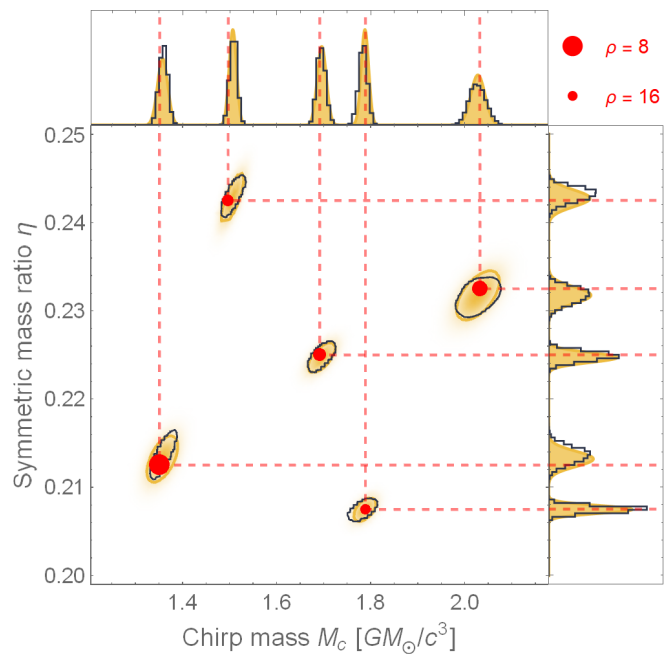


FIG. 1. Estimated (yellow) and true (black) posteriors for five test signals (red), with parameters of interest (M_c, η) and the prior $p_1(\vartheta)$. Contours in main panel are three-sigma equivalent. Posteriors in side panels are further marginalized over each parameter. Unit of M_c is one Solar mass in seconds.

PERCIVAL networks with different priors but, for the above reasons, find the most success when the priors are confined to smaller subspaces.

Our first example is a network that estimates the joint posterior of the parameters $\theta = (M_c, \eta)$, for signals distributed according to the uniform prior

$$p_1(\vartheta) \propto \mathbf{1}_{\Delta M_c \times \Delta \eta}(M_c, \eta) \delta(\chi_1) \delta(\chi_2) \mathbf{1}_{\Delta \rho}(\rho), \quad (8)$$

where the prior intervals are given by $\Delta M_c = [2.4, 4.5] \times 10^5 M_\odot$, $\Delta \eta = [0.2, 0.25]$ and $\Delta \rho = [8, 16]$. This is effectively a non-spinning three-parameter submodel. Our PERCIVAL network takes as input signal + noise coefficients β , processes them through eight hidden layers of width 1024 (with the *leaky ReLU* activation function [42] applied to each), and outputs (with linear activation) a vector of five quantities that specify a single bivariate Gaussian. Training is performed using batch gradient descent with *Adam optimization* [43] and a manually decayed learning rate. The network is fed $\sim 10^9$ examples before the loss levels off; to eliminate overfitting, we generate a new batch of 10^5 signals at every training epoch.

In Fig. 1, we compare the PERCIVAL-estimated posteriors for five test signals against the corresponding true posteriors, which are sampled through a brute-force approach that exploits the batch-generation capability of ROMAN. The trained network appears to localize the posteriors well, and to capture their near-Gaussian cor-

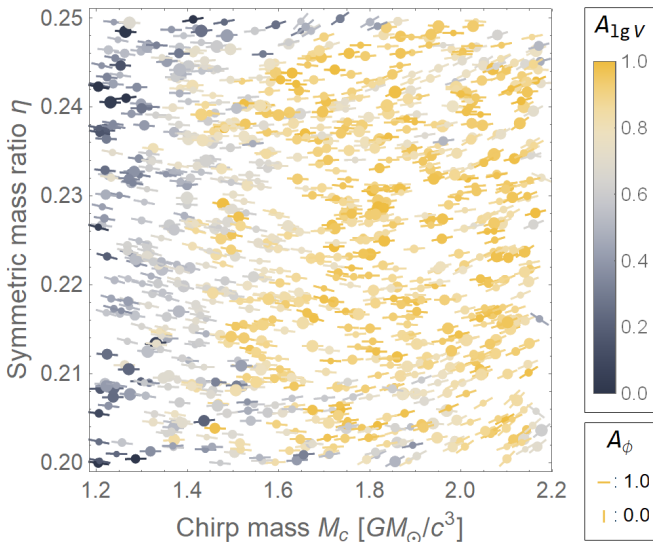


FIG. 2. Accuracy of estimated covariance matrix in terms of associated ellipse volume ($A_{\lg V}$) and orientation (A_ϕ) for 1000 test signals, using the network of Fig. 1. A value of 1 for $A_{\lg V}$ corresponds to exact prediction, and 0 to errors of more than $\times 10$; likewise, a value of 1 for A_ϕ is exact prediction, and 0 is the maximal angular error of $\pi/2$. The radius of each point is inversely proportional to the signal-to-noise ratio.

relation structure with reasonable accuracy. This statement is made more quantitative in Figs 2 and 3, where the performance of the network is assessed on larger test sets. Fig. 2 depicts the accuracy of the network-estimated posterior covariance matrix Σ , for 1000 test signals distributed according to $p_1(\vartheta)$. Each point on the plot corresponds to a single matrix, with color describing the accuracy of the associated ellipse 2-volume $V := \sqrt{\det \Sigma}$:

$$A_{\lg V} := \max \left\{ 1 - \left| \lg \frac{V}{V_{\text{true}}} \right|, 0 \right\}, \quad (9)$$

where V_{true} is obtained from the sample covariance matrix of the true posterior. The angle of the segment through each point describes the accuracy of the ellipse orientation: $A_\theta := 1 - \Delta\phi/(\pi/2)$, where $0 \leq \Delta\phi \leq \pi/2$ is the minimal angle between the principal eigenvectors of the estimated and sample covariance matrices.

For any given test signal, two overlapping factors seem to reduce network performance: (i) a smaller chirp mass, since the information content (variability) of the signal is larger in this regime, and (ii) vicinity to the (M_c, η) boundary. This latter effect is somewhat expected, since the posterior is closer to a truncated Gaussian in the case of a near-boundary signal, and the Gaussian defined by the sample covariance matrix actually tends to be a poorer fit than the (truncated) network estimate.

The distribution of network prediction errors for a test set of 5000 signals is shown in Fig. 3; the error in the mean value of each parameter $\Delta\mu(\theta)$ is quoted relative to the respective prior interval length $\Delta\theta$, while the error in each standard deviation is taken to be the quantity

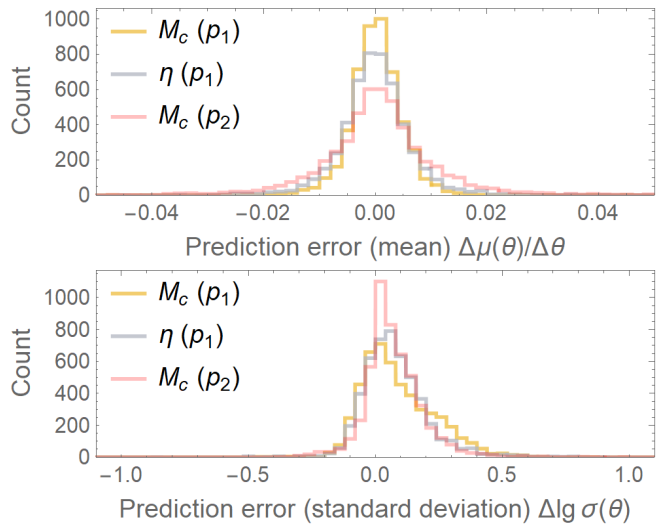


FIG. 3. Prediction error in mean values (top) and standard deviations (bottom) of posteriors for 5000 test signals, using the network of Fig. 1. Also included are results for an M_c -only network that is trained and tested on the prior $p_2(\vartheta)$.

$\Delta \lg \sigma(\theta)$ (such that a value of +1 corresponds to an overestimate of σ by a factor of ten). The network recovers the mean values at around 98% accuracy, but can overestimate the standard deviations by up to a factor of three.

In Fig. 3, we also show the error distribution of $\mu(M_c)$ and $\sigma(M_c)$ for a second PERCIVAL network that estimates the one-dimensional posterior of $\theta = M_c$, for signals distributed according to the uniform prior

$$p_2(\vartheta) \propto \mathbf{1}_{\Delta M_c \times \Delta \eta \times \Delta \chi^2 \times \Delta \rho}(M_c, \eta, \chi_1, \chi_2, \rho), \quad (10)$$

where $\Delta \chi = [-1, 1]$, and the other intervals are given as before. This network is identical to the first, except that it outputs 18 quantities specifying a three-component bivariate Gaussian mixture (five for each component, plus three weights). Even though the family of posteriors over the full five-dimensional prior space is larger and more complex, the second network yields comparable results to the first, but does have some difficulty in resolving the multimodality that arises in certain posteriors.

To show the viability of the histogram representation, we present results for a network trained on weak signals ($\rho = 2$), which exhibit posteriors with complex features. The parameter of interest is $\theta = M_c$, and the prior is

$$p_3(\vartheta) \propto \mathbf{1}_{\Delta M_c \times \Delta \eta}(M_c, \eta) \delta(\chi_1) \delta(\chi_2) \delta(\rho - 2), \quad (11)$$

where $\Delta M_c, \Delta \nu$ are given as before. While such a prior is not very relevant for gravitational-wave astronomy (since inference is unlikely to be conducted on sub-threshold sources), the PERCIVAL network is nevertheless able to estimate the highly nontrivial posteriors, due to the greater degrees of freedom in the posterior representation and the smaller prior space. Posteriors for three representative test signals are displayed in Fig. 4.

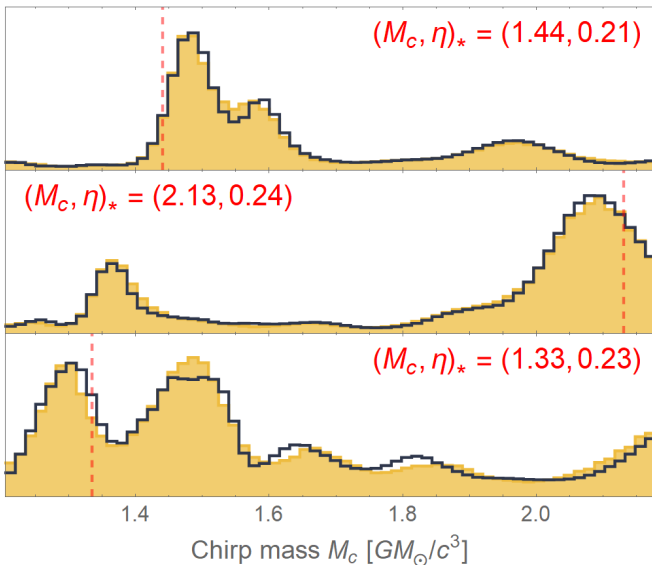


FIG. 4. Estimated (yellow) and true (black) M_c posteriors for three weak test signals (red), with the prior $p_3(\vartheta)$.

Discussion. In this Letter, we describe a proof-of-principle demonstration (PERCIVAL) of instantaneous Bayesian posterior approximation in complex inverse problems such as gravitational-wave parameter estimation, using straightforward perceptron networks trained on large signal + noise sets drawn from the assumed parameter priors and noise sampling distribution. The computational cost of parameter-space exploration is shifted from the analysis of each observed data set to the offline network-training stage, making this scheme useful for low-latency parameter estimation, or for the science-payoff characterization of future experiments. Notably, the loss function does not require likelihood evaluations, but only the true parameter values of the training examples. Thus, our scheme can be used whenever the likelihood is expensive or unknown, but forward modeling is efficient and we have access to many samples of noise.

In our examples, we leverage the hyper-efficient ROMAN forward modeling [17], which allows us to train networks over effectively infinite training sets. We find that relatively modest network architectures are able to approximate the quasi-Gaussian posteriors obtained for stronger signals, as well as the multimodal posteriors that occur at very low signal-to-noise ratios. We fully expect the accuracy of approximation to improve with network capacity and training iterations. Larger and deeper networks should also learn posteriors across broader regions of parameter space, although it may prove expedient to train separate networks for different regions.

The real-world analysis of gravitational-wave signals involves a number of complications that are not represented in our demonstration, such as multidetector data sets, the presence of *extrinsic* parameters that describe

the relative spacetime location of source and detector, and variations (or estimation error) in the noise spectral density. These are beyond the scope of this Letter, but they can be handled by a combination of strategies: simply adding extra parameters to the model, designing networks with symmetries that make them insensitive to new degrees of freedom, and transforming (e.g., time-shifting, or whitening) the input data. Last, since convolutional neural networks have been successfully trained to recognize and decode gravitational waveforms represented as strain time series, it should be possible to combine these with a posterior-generating stage analogous to PERCIVAL, providing an end-to-end mapping from detector data to Bayesian posteriors.

Acknowledgements. We are grateful to Chad Galley for sharing his expertise in reduced-order modeling, and to Chris Messenger for correspondence on his related work. We also thank Natalia Korsakova and Michael Katz for helpful conversations, and acknowledge feedback from fellow participants in the 2018 LISA workshop at the Keck Institute for Space Studies. This work was supported by the Jet Propulsion Laboratory (JPL) Research and Technology Development program, and was carried out at JPL, California Institute of Technology, under a contract with the National Aeronautics and Space Administration. © 2019 California Institute of Technology. U.S. Government sponsorship acknowledged.

* Alvin.J.Chua@jpl.nasa.gov

† Michele.Vallisneri@jpl.nasa.gov

- [1] P. Gregory, *Bayesian Logical Data Analysis for the Physical Sciences: A Comparative Approach with Mathematica® Support* (Cambridge University Press, 2005).
- [2] LIGO Scientific Collaboration and Virgo Collaboration and others, arXiv:1811.12907 (2018).
- [3] B. Abbott, R. Abbott, T. Abbott, S. Abraham, F. Acernese, K. Ackley, C. Adams, R. Adhikari, V. Adya, C. Affeldt, *et al.*, arXiv:1811.12940 (2019).
- [4] J. Creighton and W. Anderson, *Gravitational-Wave Physics and Astronomy: An Introduction to Theory, Experiment and Data Analysis*, Wiley Series in Cosmology (Wiley, 2011).
- [5] M. Hannam, P. Schmidt, A. Bohé, L. Haegel, S. Husa, F. Ohme, G. Pratten, and M. Pürrer, *Phys. Rev. Lett.* **113**, 151101 (2014).
- [6] Y. Pan, A. Buonanno, A. Taracchini, L. E. Kidder, A. H. Mroué, H. P. Pfeiffer, M. A. Scheel, and B. Szilágyi, *Phys. Rev. D* **89**, 084006 (2014).
- [7] J. Blackman, S. E. Field, C. R. Galley, B. Szilágyi, M. A. Scheel, M. Tiglio, and D. A. Hemberger, *Phys. Rev. Lett.* **115**, 121102 (2015).
- [8] S. A. Usman, A. H. Nitz, I. W. Harry, C. M. Biwer, D. A. Brown, M. Cabero, C. D. Capano, T. D. Canton, T. Dent, S. Fairhurst, *et al.*, *Classical and Quantum Gravity* **33**, 215004 (2016).

- [9] C. Messick, K. Blackburn, P. Brady, P. Brockill, K. Cannon, R. Cariou, S. Caudill, S. J. Chamberlin, J. D. E. Creighton, R. Everett, *et al.*, Phys. Rev. D **95**, 042001 (2017).
- [10] M. Vallisneri, Phys. Rev. D **77**, 042001 (2008).
- [11] I. Goodfellow, Y. Bengio, and A. Courville, *Deep Learning* (MIT Press, 2016).
- [12] S. S. Haykin, *Neural Networks: A Comprehensive Foundation* (Prentice Hall, 1999).
- [13] C. de Troyes, B. Raffel, and J. J. Duggan, *Perceval: The Story of the Grail* (Yale University Press, 1999).
- [14] B. P. Abbott *et al.*, The Astrophysical Journal **875**, 161 (2019).
- [15] N. Christensen and R. Meyer, Phys. Rev. D **58**, 082001 (1998).
- [16] K. Danzmann *et al.*, ArXiv e-prints (2017), arXiv:1702.00786 [astro-ph.IM].
- [17] A. J. K. Chua, C. R. Galley, and M. Vallisneri, Phys. Rev. Lett. **122**, 211101 (2019).
- [18] S. E. Field, C. R. Galley, F. Herrmann, J. S. Hesthaven, E. Ochsner, and M. Tiglio, Phys. Rev. Lett. **106**, 221102 (2011).
- [19] S. E. Field, C. R. Galley, J. S. Hesthaven, J. Kaye, and M. Tiglio, Phys. Rev. X **4**, 031006 (2014).
- [20] P. Cañizares, S. E. Field, J. R. Gair, and M. Tiglio, Phys. Rev. D **87**, 124005 (2013).
- [21] Y. LeCun and Y. Bengio, in *The Handbook of Brain Theory and Neural Networks*, edited by M. A. Arbib (MIT Press, Cambridge, MA, USA, 1998) pp. 255–258.
- [22] T. Gebhard, N. Kilbertus, G. Parascandolo, I. Harry, and B. Schölkopf, in *Workshop on Deep Learning for Physical Sciences (DLPS) at the 31st Conference on Neural Information Processing Systems (NIPS)* (2017).
- [23] D. George and E. A. Huerta, Phys. Rev. D **97**, 044039 (2018).
- [24] D. George and E. Huerta, Physics Letters B **778**, 64 (2018).
- [25] H. Gabbard, M. Williams, F. Hayes, and C. Messenger, Phys. Rev. Lett. **120**, 141103 (2018).
- [26] X. Fan, J. Li, X. Li, Y. Zhong, and J. Cao, Science China Physics, Mechanics & Astronomy **62**, 969512 (2019).
- [27] H. Nakano, T. Narikawa, K.-i. Oohara, K. Sakai, H.-a. Shinkai, H. Takahashi, T. Tanaka, N. Uchikata, S. Yamamoto, and T. S. Yamamoto, Phys. Rev. D **99**, 124032 (2019).
- [28] A. Rebei, E. A. Huerta, S. Wang, S. Habib, R. Haas, D. Johnson, and D. George, Phys. Rev. D **100**, 044025 (2019).
- [29] H. Shen, E. Huerta, and Z. Zhao, arXiv:1903.01998 (2019).
- [30] T. D. Gebhard, N. Kilbertus, I. Harry, and B. Schölkopf, arXiv:1904.08693 (2019).
- [31] P. G. Krastev, arXiv:1908.03151 (2019).
- [32] A. Mytidis, A. A. Panagopoulos, O. P. Panagopoulos, A. Miller, and B. Whiting, Phys. Rev. D **99**, 024024 (2019).
- [33] C. Dreissigacker, R. Sharma, C. Messenger, R. Zhao, and R. Prix, Phys. Rev. D **100**, 044009 (2019).
- [34] F. Morawski, M. Bejger, and P. Ciecielag, arXiv:1907.06917 (2019).
- [35] A. L. Miller, P. Astone, S. D’Antonio, S. Frasca, G. Intini, I. La Rosa, P. Leaci, S. Mastrogiovanni, F. Muciaccia, A. Mitidis, C. Palomba, O. J. Piccinni, A. Singhal, B. F. Whiting, and L. Rei, arXiv e-prints, arXiv:1909.02262 (2019), arXiv:1909.02262 [astro-ph.IM].
- [36] H. Gabbard, C. Messenger, I. S. Heng, F. Tonolini, and R. Murray-Smith, arXiv preprint (2019).
- [37] F. Tonolini, A. Lyons, P. Caramazza, D. Faccio, and R. Murray-Smith, arXiv preprint arXiv:1904.06264 (2019).
- [38] D. W. Ruck, S. K. Rogers, M. Kabrisky, M. E. Oxley, and B. W. Suter, IEEE Transactions on Neural Networks **1**, 296 (1990).
- [39] E. A. Wan, IEEE Transactions on Neural Networks **1**, 303 (1990).
- [40] D. Pollard, *A User’s Guide to Measure Theoretic Probability*, Cambridge Series in Statistical and Probabilistic Mathematics (Cambridge University Press, 2002).
- [41] K. G. Arun, A. Buonanno, G. Faye, and E. Ochsner, Phys. Rev. D **79**, 104023 (2009).
- [42] A. L. Maas, A. Y. Hannun, and A. Y. Ng, in *Proceedings of the 30th International Conference on Machine Learning* (2013).
- [43] D. P. Kingma and J. Ba, ArXiv e-prints (2014), arXiv:1412.6980.